

## Application of Residual Correction Method on non-Fourier Heat Transfer for Sphere with Time-Dependent Boundary Condition

Po-Jen Su<sup>1</sup>, Cha'o-Kung Chen<sup>1</sup>

**Abstract:** The residual correction method is used to predict the temperature distribution of non-Fourier heat transfer with time-dependent boundary condition. The approximate solution of temperature field is obtained by the residual correction method based on the maximum principle in combination with the finite difference method, making it easier and faster to obtain upper and lower approximations of exact solutions, and even can provide clear definitions of the maximum error bounds of the approximate solutions. The proposed method is found to be an effective numerical method with satisfactory accuracy.

**Keywords:** residual correction method, maximum principle, non-Fourier heat transfer, time-dependent boundary conduction

### Nomenclature

$k$  thermal conductivity (W/m·K)  
 $\mathbf{q}$  heat flux (W/m<sup>2</sup>)  
 $T$  distribution temperature of media (K)  
Tr ratio of  $\tau_T$  to  $\tau_q$

### Greek symbols

$\alpha$  thermal diffusivity (m<sup>2</sup>/s)  
 $\tau_q$  phase lag of the heat flux vector (relaxation time) (s)  
 $\tau_T$  phase lag of the temperature gradient (relaxation time) (s)

---

<sup>1</sup> Department of Mechanical Engineering, National Cheng Kung University, Tainan, Taiwan 70101, R.O.C.

Email: ckchen@mail.ncku.edu.tw

Tel: +886-62757575#62140

**Superscripts**

- $\sim$  approximate function  
 $\cap, \cup$  upper and lower approximate solutions  
 $n$  value at previous grid point of time or value of the last iteration

**Subscripts**

- $i, j, k$  serial number of the calculation grid point

**1 Introduction**

With the progress of technology, modern film deposition and patterning techniques can produce structures with dimensions in micrometers even to nanometers. This has led to a trend towards the miniaturization of high-tech industrial products, with the precision or size of key components being reduced to the micron or nanometer level. Although such a reduction of device size enhances the switching speed of the device, but at a cost of high thermal loading. These developments have driven the extreme miniaturization of electronic devices, (e.g., nano-scaled electronic structures), leading to increasing concerns about steady and transient thermal behaviors which can lead to errors in the classical Fourier heat transfer analysis [Vermeersch and Mey (2008), Xu and Guo (1995)]. In recent years, considerable research has been devoted to non-Fourier heat transfer phenomena. Maxwell (1867) and Nernst (1918) suggested through theoretical observations that, given low temperatures with properly chosen conductors, heat may have sufficient *inertia* to result in oscillatory discharge. Peshkov (1944) measured the propagation velocity of heat flux in liquid helium at 1.4 K to be 19 m/s, contradicting Fourier's (FO) law of heat conduction. Taitel (1972) hypothesized that the transient temperature at the middle location of a slab with constant-temperature heat sources at both ends can be higher than that of the sources, called *Taitel's paradox*. Based on classical Fourier heat conduction theory, the heat flux vector ( $\mathbf{q}$ ) has a linear relation with the temperature gradient ( $\nabla T$ ) which implies the propagation speed of the thermal wave is infinite. That is to say, any thermal disturbance exerted on a body is instantaneously felt through the whole body. To eliminate the paradox of an infinite thermal wave speed which contradicts Einstein's theory of relativity and thus provide a theory to explain the experimental data on "second sound" in liquid and solid helium at low temperatures [Chester (1963), Brown, Chung and Matthews (1966)], Cattaneo (1958) and Vernotee (1961) independently postulated a constitutive relation between the heat flux vector ( $\mathbf{q}$ ) and temperature gradient ( $\nabla T$ ) in solids, so-called

CV wave model, as

$$\mathbf{q} + \tau_q \frac{\partial \mathbf{q}}{\partial t} = -k \nabla T \quad (1)$$

where  $\tau_q$  indicates the observed time-lag, the so-called relaxation time. Inserting Eq. (1) into the energy conservation equation yields a hyperbolic heat transport equation. More recently, Tzou (1997) proposed the dual-phase-lag model (DPL) to interpret the precedence assumption of the temperature gradient (cause) to precede the heat flux vector (effect) or the heat flux vector (cause) to precede the temperature gradient (effect) in the transient heat transfer process. Mathematically, this can be represented by

$$\mathbf{q}(\mathbf{r}, t + \tau_q) = -k \nabla T(\mathbf{r}, t + \tau_T) \quad (2)$$

Two relaxation times  $\tau_T$  and  $\tau_q$  are both regarded as the intrinsic thermal or structural properties of the material. The former is attributed to micro-structural interactions such as phonon–electron interaction or phonon scattering, and is termed the phase-lag of the temperature gradient. The latter is interpreted as the relaxation time accounting for the fast-transient effects of thermal inertia, and is called the phase-lag of the heat flux. For  $\tau_q < \tau_T$  the temperature gradient established across the material volume is as a result of the heat flow, implying that the heat flux vector is the cause and the temperature gradient is the effect. For  $\tau_q > \tau_T$ , heat flow is induced by the earlier-established temperature gradient, implying that the temperature gradient is the cause, while the heat flux vector is the effect. In the absence of the phase lag of the temperature gradient  $\tau_T = 0$ , Eq. (2) reduces to the CV wave model. In addition to low temperature (i.e., temperatures near absolute zero) applications, non-Fourier theories have attracted more attention in the engineering sciences due to their application in the extreme miniaturization of devices, high heat flux conduction, extreme thermal gradients, very short time behavior such as the annealing of semiconductors and laser surgery in biomedical engineering. Moreover, experimental and theoretical studies on these applications have been reported by numerous investigators [Baeri et al. (1979), Kaminiski (1990), Mitra et al. (1995), Xu and Guo (1995), Saedodin and Torabi (2010), Ni et al. (2011), Banerjee et al. (2005), Hong et al. (2011)]. Comprehensive literature surveys of non-Fourier heat transfer before 1980s can be found in reviews by Joseph and Preziosi (1989). It is now accepted that in the above mentioned situations, Fourier's heat diffusion theory loses accuracy and the non-Fourier effect becomes more reliable in describing the diffusion process and predicting the temperature distribution.

Various analytical and numerical solutions to the non-Fourier heat transfer equation regarding time-dependent boundary conditions can be found in the literature.

Heidarinejad, Shirmohammadi and Maerefat (2008) analytically studied the hyperbolic heat conduction in a plane slab, an infinitely long solid cylinder and a solid sphere with a time dependent boundary heat flux based on the separation of variables method and Duhamel's principle. Frankel, Vick and Ozisik (1985) have demonstrated the hyperbolic heat conduction in the finite thickness slab to a pulsed surface heat flux, resulting in a finite speed of propagation of the thermal waves. Tang and Araki (1996) have analytically investigated the non-Fourier effects in a finite medium subjected to a periodic boundary heat flux condition using the hyperbolic heat conduction model. Barletta and Zanchini (1996) studied the temperature profile in a finite medium imposed on a boundary condition of the exponentially time decaying heat flux. Liu and Chen (2004) presented a numerical solution for the temperature distribution of hyperbolic heat conduction in a finite slab with pulsed boundary conditions.

Flow and heat transfer frequently appear in various manifestations in engineering and scientific research, including air-conditioning and electronic cooling, which often entail various problems requiring exact solutions, i.e., the solution of the governing equation under the given boundary and initial conditions. Finding exact solutions for these various governing equations was only possible in a very limited number of cases. In other words, it is usually difficult to find exact solutions for complex geometric shapes even with nonlinear equations and non-homogeneous boundary conditions in engineering applications or scientific research under the given initial and boundary conditions. Given this difficulty to obtain analytic solutions for such complex geometric shapes with non-homogeneous boundary conditions, it is only possible to find their approximate solutions through certain numerical methods, including the Residual Correction Method. This study discusses the time dependent boundary conditions, which cannot be used to solve the problem directly.

Past studies have verified that the error margin between approximate solution and exact solution usually decreases with the increase of grid points or the numbers of approximate functions which require more memory space and calculation time. However, it is still impossible to completely determine the accuracy of the approximate solution. As early as 1967, Protter proposed the concept of the maximum principle which explains the relationship between the solution and the residual of a differential equation and can therefore be used to find the upper and lower approximate solutions of the exact solutions of some differential equations. However, until recently this concept had not been broadly applied in numerical methods, as this approach includes a programming problem of mathematical inequalities that requires time-consuming calculations. In recent years, some scholars have made attempts to simplify the calculating procedure. Lee et al. (2002) successfully used genetic

algorithms to apply simplified equations reliant on trial functions to handle programming problems generated in the optimization process. Wang and Hu (2008) proposed a method to determine monotonicity in individual differential equations. Wang (2006; 2007; 2010) and Cheng et al. (2009) used the cubic spline approximation to discretize the differential equations into the programming problems. The inequality-constraint programming problems can then be converted into simple iterative equations based on the residual correction concept, thus significantly improving the efficiency of obtaining solutions. Tang et al. (2010) and Peng et al. (2012) extended previous studies for separate applications to non-Fourier problems for fins and the laser heating process. They applied the finite difference to discretize the equation, converting the differential equation into a programming problem, and then incorporated the residual correction method to obtain the upper and lower approximate solutions. Their study showed that incorporating the residual correction method into the nonlinear iterative procedure of the finite difference can make it easier and faster to obtain approximate solutions.

This paper studies the non-Fourier heat transfer problem for a micro-sphere with a time-dependent heat flux boundary via the residual correction method based on maximum principles in differential equations. The advantage of this method is that the upper and lower approximate solutions obtained can restrict the exact solution in a known region, thus it can be used to estimate the range of the maximum possible error between the approximate solution and the exact solution, avoiding a blind increase of calculation grid points to obtain more accurate approximate solutions. The influences of time-dependent boundary, radiation boundary conditions and short pulsed laser parameters are examined.

## **2 Mathematical Preliminaries**

### ***2.1 Maximum Principle for Differential Equations***

The maximum principle for differential equations is a generalization of basic problems in calculus to describe a continuously differentiable function as having its maximum value at one endpoint of an interval if it satisfies the inequality  $f''(x) > 0$  on the interval. That is to say, if a function satisfies a differential inequality in a domain and obtains its maximum value on the boundaries of the domain, we can say that the differential equation satisfies the maximum principle for differential equations with monotonicity. The approach is based on the concept of maximum principle to build up the residual of differential equations and thus obtain the upper and lower approximate solutions. At first, assume a differential equation in the form below:

$$R_{\tilde{\theta}}(x) = F(x, \tilde{u}, \tilde{u}_x, \tilde{u}_{xx}) - f(x) \quad \text{in } D \tag{3}$$

Boundary conditions satisfy

$$R_{\tilde{\theta}}(x) = g(x) - \tilde{\theta}(x) \quad \text{on } \partial D \tag{4}$$

where the function  $R_{\tilde{\theta}}(x)$  is known as the residual value function of the approximate function  $\tilde{\theta}(x)$  of the differential equation in the domain  $D$  or on the boundaries  $\partial D$ . Assuming that the approximate solutions are defined in the calculation domain and are continuous to second derivatives, if

$$\frac{\partial R}{\partial \theta} \leq 0 \quad \text{in } D \tag{5}$$

then, if and only if the following relationship between the residual relation and approximate functions holds true

$$R_{\tilde{\theta}}(x) \geq R_{\theta}(x) = 0 \geq R_{\hat{\theta}}(x) \quad \text{on } D \cup \partial D \tag{6}$$

the approximate solutions will have the following relation with the exact solution:

$$\tilde{\theta}(x) \leq \theta(x) \leq \hat{\theta}(x) \quad \text{on } D \cup \partial D \tag{7}$$

where  $\tilde{\theta}(x)$  and  $\hat{\theta}(x)$  are respectively known as the lower and upper approximate solutions of the exact solution  $\theta(x)$ . A differential equation with such relations is considered monotonic.

## 2.2 Residual Correction Steps

Use the finite difference method to discretize and reformulate the residual relation into the following expression:

$$R_{r,i,j,k}(t, x, y, z) = - \left( L[\theta]_{r,i,j,k}^{n+1} + N[\theta]_{r,i,j,k}^n \right) + f_{r,i,j,k} \tag{8}$$

where  $L$  is the linear operator and  $N$  is the nonlinear operator, the superscript  $n$  is the iterative times, and the subscript  $r, i, j, k$  is the serial number of the grid points after discretizing.

Then, transfer the expression into an iterative equation with residual correction to avoid complex calculations:

$$-\left(L[\theta]_{r,i,j,k}^{n+1} + N[\theta]_{r,i,j,k}^n\right) + f_{r,i,j,k} = \begin{matrix} \max \\ \min \end{matrix} \left(\Delta R_{r,i,j,k}^n(t, x, y, z)\right) \quad (9)$$

where  $\Delta R_{r,i,j,k}^n(t, x, y, z)$  indicates the residual distribution function of the last calculation results on adjacent subintervals of grid points. It can be expanded as follows by using the Taylor series at the grid points:

$$\Delta R_{r,i,j,k}(t, x, y, z) = \sum_{s=1}^{\infty} \sum_{p=1}^{\infty} \sum_{q=1}^{\infty} \sum_{l=1}^{\infty} \frac{\partial R_{r,i,j,k}(t, x, y, z)}{\partial t^s \partial x^p \partial y^q \partial z^l} \frac{(t-t_r)^s (x-x_i)^p (y-y_j)^q (z-z_k)^l}{s!p!q!r!} \quad (10)$$

$$(t_r - \Delta t) \leq t \leq (t_r) \quad (x_i - \Delta x) \leq x \leq (x_i + \Delta x)$$

$$(y_j - \Delta y) \leq y \leq (y_j + \Delta y), \quad (z_k - \Delta z) \leq z \leq (z_k + \Delta z)$$

Then, the residual values on the adjacent subintervals of the grids can be ensured to be all positive or all negative by the residual values at the calculation grids which are corrected by indentifying the maximum and minimum of residual values on these intervals.

The convergence criterion applied in the present study is the relative error convergence as defined by the following equations:

$$E_{\theta} = \left| \frac{\tilde{\theta}_i^{n+1} - \tilde{\theta}_i^n}{\tilde{\theta}_i^n} \right| \leq \varepsilon, \quad i = 0, 1, \dots, N_i \quad (11)$$

### 3 Model Description

Consider a radial one-dimensional non-Fourier heat conduction process in a hollow sphere with inner and outer radii  $r_i$  and  $r_o$ , respectively as shown in Fig. 1, composed of an isotropic heat conduction material with constant thermal properties. From time  $t = 0$  its inner surface is irradiated by a  $Q$ -switched laser source with power  $Q(t) = \frac{Q_0}{4\pi r_i^2 t_p} \exp\left(-\frac{t}{t_p}\right)$  where  $t_p$  is the characteristic time of the laser pulse and  $\frac{Q_0}{4\pi r_i^2}$  is the laser intensity defined as the total energy ( $Q_0$ ) carried by laser pulse per unit inner spherical surface area. By modulating the value of  $t_p$ , the laser pulse with different time durations can be obtained as in Fig. 2.

The pulse energy is assumed to be absorbed at the inner surface of the sphere. The thermal disturbance is caused by a sudden change in heat flux on the sphere's inner

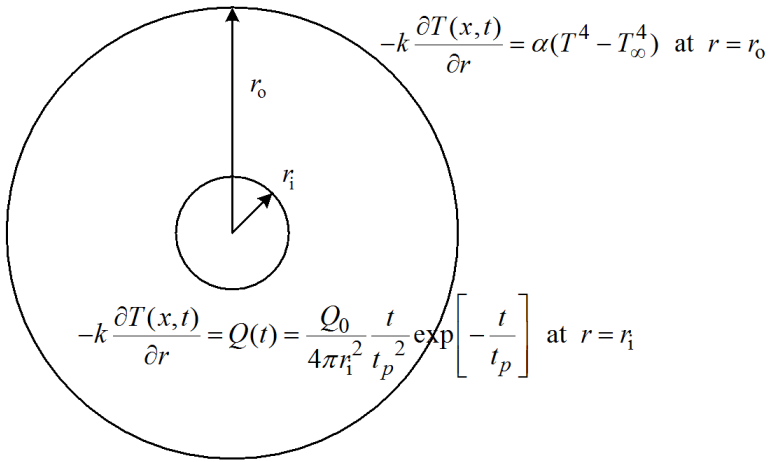


Figure 1: Computation domain

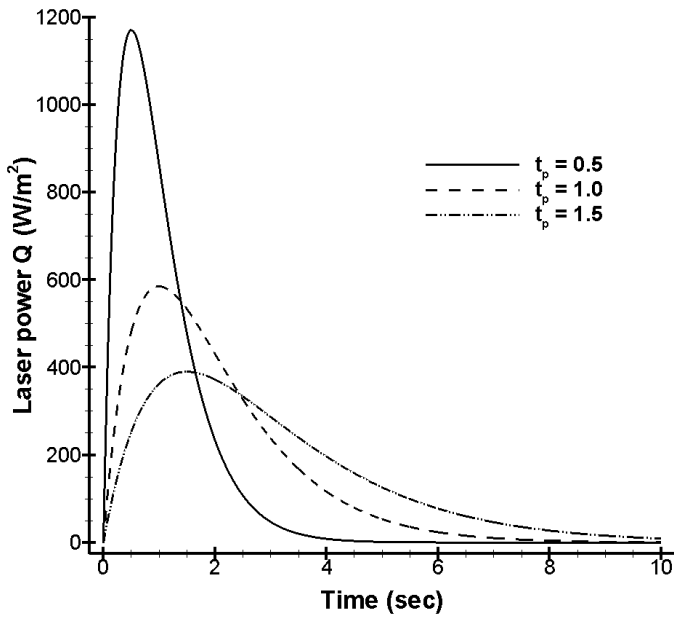


Figure 2: Temporal profile of the heating laser with different pulse durations

surface while the outer surface is considered with the radiation boundary condition. No heat source is involved and heat convection and radiation are disregarded. Therefore, the non-Fourier heat conduction equation is formulated as follows

$$\frac{\partial^2 T}{\partial r^2} + \frac{2}{r} \frac{\partial T}{\partial r} + \tau_T \frac{\partial}{\partial t} \left( \frac{\partial^2 T}{\partial r^2} + \frac{2}{r} \frac{\partial T}{\partial r} \right) = \frac{1}{\alpha} \frac{\partial T}{\partial t} + \frac{\tau_q}{\alpha} \frac{\partial^2 T}{\partial t^2} \quad (12)$$

For the considered situation, the boundary conditions are introduced as

$$-k \frac{\partial T(r,t)}{\partial r} \Big|_{r=r_i} = Q(t) = \frac{Q_0}{4\pi r_i^2} \frac{t}{t_p^2} \exp\left(-\frac{t}{t_p}\right) \quad (13)$$

$$-k \frac{\partial T(r,t)}{\partial r} \Big|_{r=r_o} = \sigma (T^4 - T_\infty^4) \quad (14)$$

and initial conditions are assumed to be

$$T(r,0) = T_0 \quad ; \quad \frac{\partial T(r,0)}{\partial t} = 0$$

The residual correction relation is established for the governing Eq. (12) in the form of

$$R(r,t) = T_{rr} + \frac{2}{r} T_r + \tau_T \left( T_{trr} + \frac{2}{r} T_{tr} \right) - \frac{1}{\alpha} T_t - \frac{\tau_q}{\alpha} T_{tt} \quad (15)$$

Before continuing the calculation steps, the maximum principle is applied to determine whether Eq. (15) is monotonic.

$$\frac{\partial R}{\partial T} = \frac{\partial}{\partial T} \left( T_{rr} + \frac{2}{r} T_r + \tau_T \left( T_{trr} + \frac{2}{r} T_{tr} \right) - \frac{1}{\alpha} T_t - \frac{\tau_q}{\alpha} T_{tt} \right) = 0 \quad (16)$$

If the maximum principal is satisfied, the required condition is:

$$\frac{\partial R}{\partial T} \leq 0 \quad (17)$$

Thus Eq. (17) holds and the monotonicity exists.

The residual correction method is used in combination with the finite difference method of implicit scheme to discretize Eq. (12), followed by the addition of a residual correction at every grid point. An iterative relation will then be generated in the form of

$$\begin{aligned}
 & \left[ \frac{1}{(\Delta r)^2} - \frac{1}{r_i \Delta r} + \frac{\tau_r}{2\Delta t (\Delta r)^2} - \frac{\tau_r}{2r_i \Delta t \Delta r} \right] T_{i-1}^{n+1} + \left[ -\frac{2}{(\Delta r)^2} - \frac{\tau_r}{\Delta t (\Delta r)^2} - \frac{1}{2\alpha \Delta t} - \frac{\tau_q}{\alpha (\Delta r)^2} \right] T_i^{n+1} \\
 & + \left[ \frac{1}{(\Delta r)^2} + \frac{1}{r_i \Delta r} + \frac{\tau_r}{2\Delta t (\Delta r)^2} + \frac{\tau_r}{2r_i \Delta t \Delta r} \right] T_{i+1}^{n+1} \\
 & = \left[ -\frac{2\tau_q}{\alpha (\Delta r)^2} \right] T_i^n + \left[ \frac{\tau_r}{2(\Delta t)(\Delta r)^2} - \frac{\tau_r}{2r_i(\Delta t)(\Delta r)} \right] T_{i-1}^{n-1} + \left[ -\frac{\tau_r}{\Delta t (\Delta r)^2} - \frac{1}{2\Delta t} + \frac{\tau_q}{\alpha (\Delta r)^2} \right] T_i^{n-1} \\
 & + \left[ \frac{\tau_r}{2\Delta t (\Delta r)^2} + \frac{\tau_r}{2r_i \Delta t \Delta r} \right] T_{i+1}^{n-1} - \frac{\text{Max}(0, -R_t^n \Delta t)}{\text{Min}} - \frac{\text{Max}(R_r^n \Delta r, -R_r^n \Delta r)}{\text{Min}}
 \end{aligned} \tag{18}$$

The finite-difference method is used to discretize the initial and boundary conditions,

$$T_i^0 = 0 \tag{19}$$

$$T_i^0 = T_i^2 \tag{20}$$

$$T_0^{n+1} = T_2^{n+1} + \frac{2\Delta r}{k} \frac{Q_0}{4\pi r_i^2} \frac{t^{n+1}}{t_p^2} \exp \left[ -\frac{t^{n+1}}{t_p} \right] \tag{21}$$

$$T_{N_i+1}^{n+1} = T_{N_i-1}^{n+1} - \frac{2\sigma \Delta r}{k} \left\{ [T_{N_i}^{n+1}]^4 - T_\infty^4 \right\} \tag{22}$$

For the above expression, if two variables  $r$  and  $t$  of Eq. (15) are partially differentiated, and the differential terms of a higher order,  $T_{rrr}$  and  $T_{ttt}$  are neglected, then  $R_r$  and  $R_t$  can be expressed as

$$R_r = (-2r^{-2}T_r + 2r^{-1}T_{rr}) + \tau_T (-2r^{-2}T_{tr} + 2r^{-1}T_{trr}) - \alpha^{-1}T_{rt} - \tau_q \alpha^{-1}T_{rtt} \tag{23}$$

$$R_t = T_{trr} + 2r^{-1}T_{tr} + \tau_T (T_{trr} + 2r^{-1}T_{tr}) - \alpha^{-1}T_{tt} \tag{24}$$

#### 4 Results and Discussion

To verify the applicability of residual correction method for spherical coordinates, this paper refers to parameter settings selected by Pourmohamadian et al. (2007) as a basis for comparison. Their work developed a heat transfer regime map for

a transient symmetrical solid sphere without source terms, but with a prescribed constant temperature at the surface. As seen in Fig. 3, using the method developed by Pourmohamadian et al. (2007), the temperature profiles at the interior nodes are placed between the upper and lower approximate solutions. The results are also in good agreement with the analytical solution.

Figure 4 illustrates the temperature distributions of various numbers of grid points for the case in Fig. 1 of the DPL model. The inner radius  $r_i$  is 0.001 m. The mean values of the upper and lower approximate solutions in all cases are close to the analytical solution, although the range between the upper and lower solutions narrows as the grid number increases. Therefore, fewer grid points can be adopted for the efficiency calculation. But the subsequent simulation still uses  $N = 1600$  to prevent the intertwining of curves. Figure 5 shows the temperature profiles along the radial direction for the different heat transfer models. As expected, the curve of CV model drops sharply due to the nature of the equation. The CV model induces a thermal wave and leads to a discontinuous temperature response. The temperature profiles of the DPL model predicted similar behavior as an FO model but is reduced due to its nature of the time lag. The ratio of  $\tau_T$  to  $\tau_q$  varies from 0.005 to 0.95 for the DPL model is depicted in Fig. 6, which shows the temperature prediction with increasing time. It shows that, following the  $Tr$  decrease, the nature of the time lag was revealed. As the relaxation time of phase lag of the temperature gradient approaches zero (0.005 in this case), the relation is reduced to the CV model. By setting it close to one, (0.95 in this case), the solution obviously is reduced to the FO model, and the time lag phenomena vanish. In the case of  $\tau_T = \tau_q$ , not necessarily equal to zero, Eq. (12) can be rearranged into the following form

$$\left(\frac{\partial^2 T}{\partial r^2} + \frac{2}{r} \frac{\partial T}{\partial r} - \frac{1}{\alpha} \frac{\partial T}{\partial t}\right) + \tau_q \frac{\partial}{\partial t} \left(\frac{\partial^2 T}{\partial r^2} + \frac{2}{r} \frac{\partial T}{\partial r} - \frac{1}{\alpha} \frac{\partial T}{\partial t}\right) = 0 \tag{25}$$

For a homogeneous initial temperature, it has a general solution

$$\frac{\partial^2 T}{\partial r^2} + \frac{2}{r} \frac{\partial T}{\partial r} - \frac{1}{\alpha} \frac{\partial T}{\partial t} = 0 \tag{26}$$

which is the classical diffusion equation, i.e., Fourier’s law.

Figure 7 shows the temperature distributions versus spatial coordinates for various relaxation time ratios. It shows the temperature distribution decreases suddenly near the inner surface, especially as the relaxation time ratio,  $Tr$ , approaches zero. This is caused by the effects of heat transfer lag, which induces the so-called thermal wave phenomena.

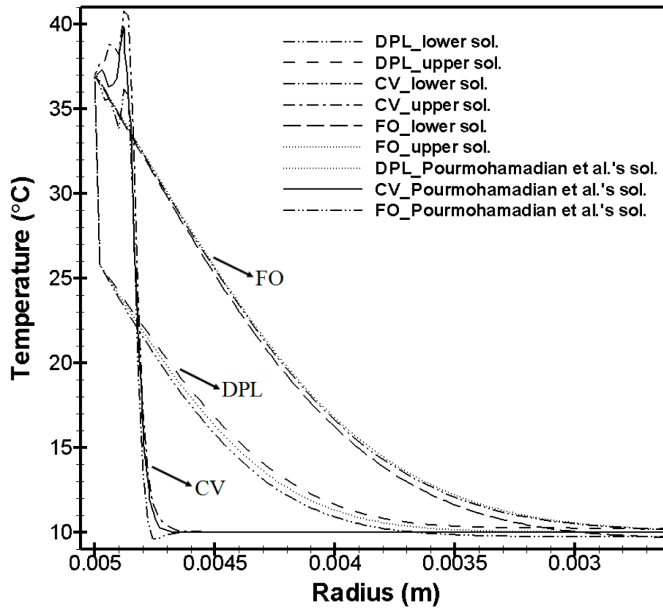


Figure 3: Comparison between present and Pourmohamadian et al.'s results (2007) for the FO, CV and DPL models

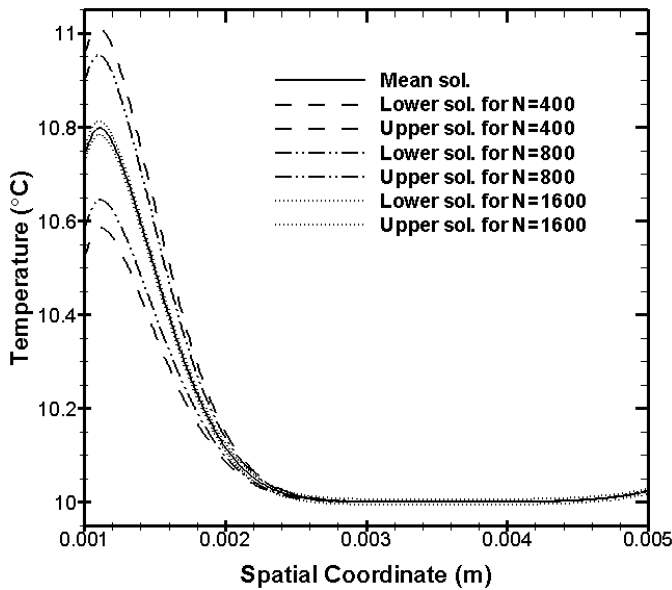


Figure 4: Upper and lower solutions of temperature distributions for various grid number values for DPL model ( $t=1.0$  sec;  $\tau_p=0.01$  sec)

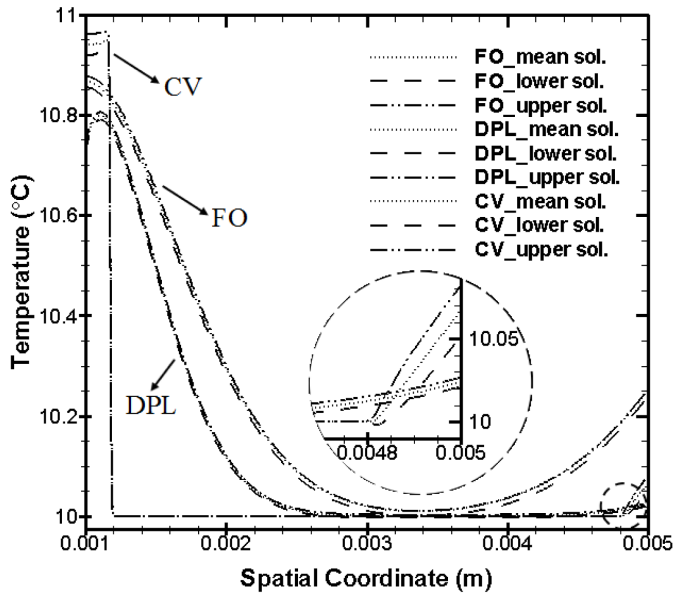


Figure 5: Comparison of temperature distributions for various models after 1 sec.

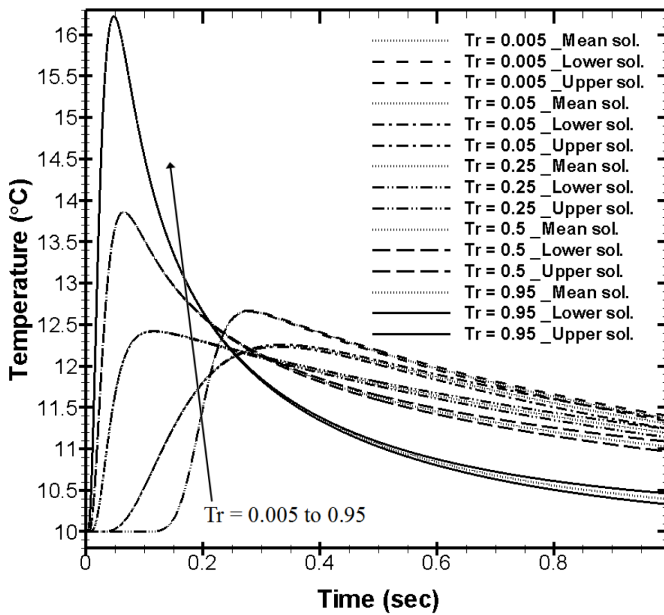


Figure 6: Comparison of upper and lower solutions for temperature distributions versus time for various relaxation time ratios

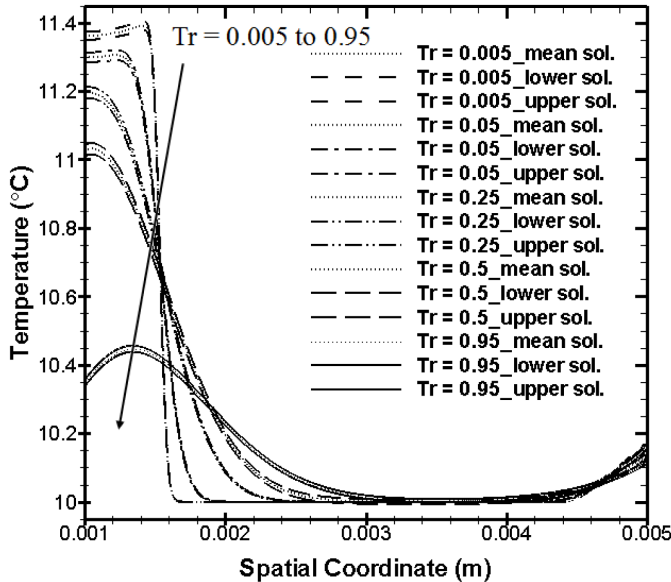


Figure 7: Upper and lower solutions for temperature distributions versus spatial coordinates for various relaxation time ratios. ( $t=1\text{sec}$ )

## 5 Conclusion

Based on the validation by the non-Fourier heat transfer for hollow spheres with a time-dependent boundary on the inner surface of a hollow sphere, the proposed residual correction method is found to effectively identify upper and lower approximate solutions. The residual correction values at every grid point can be handled simultaneously in the solution process without requiring additional iterations.

A comparison of various relaxation time ratios for the DPL heat transfer model in a symmetrical hollow sphere solved numerically with the residual correction method produces the upper and lower approximate solutions and the error range. The simulation shows the effect of the FO, CV and DPL models. CV is found to predict higher temperatures than the FO model for the present heat flux boundary condition, while the DPL predicts lower temperatures.

The results show that different heat transfer models or even different parameter values may change the error range of approximate solutions, even if the relevance of these factors is complex. The method proposed is capable of properly identifying the range within which exact solutions are expected to exist. In addition to producing mean approximate solutions with acceptable numerical accuracy, the method allows us to estimate the range of maximum possible error between the approxi-

mate and exact solutions and to avoid a blind increase of calculation grid points to obtain more accurate approximate solutions.

### **Acknowledgement**

Thanks for the subsidy of the Outlay NSC 101-2221-E-006 -092 -MY2 given by National Science Council, the Republic of China, to help us finish this special research successfully.

### **References**

- Baeri, P.; Campisano, S.U.; Foti, G.; Rimini, E.** (1979): A melting model for pulsing-laser annealing of implanted semiconductors, *Journal of Applied Physics*, Vol. 50, No. 2, pp. 788-797.
- Banerjee, A.; Ogale, A.A.; Das, C.; Mitra, K.** (2005): Temperature distribution in different materials due to short pulse laser irradiation, *Heat Transfer Engineering*, Vol. 26, No. 8, pp. 41-49.
- Barletta, A.; Zanchini, E.** (1996): Non-Fourier heat conduction in a plane slab with prescribed boundary heat flux, *Heat and mass transfer*, Vol. 31, pp. 443-450.
- Brown, J.B.; Chung, D.Y.; Matthews, P.W.** (1966): Heat pulses at low temperatures, *Physics Letters*, Vol. 21, No. 3, pp. 241-243.
- Cattaneo, C.** (1958): A form of heat conduction equation which eliminates the paradox of instantaneous propagation, *Compte Rendus Acad. Sci.*, Vol. 247, pp. 431-433.
- Cheng, C.Y.; Chen, C.K.; Yang, Y.T.** (2009): Numerical study of residual correction method applied to non-linear heat transfer problem, *CMES: Computer Modeling in Engineering & Science*, Vol. 44, No. 3, pp. 203-218.
- Chester, M.** (1963): Second sound in solids, *Physical Review*, Vol.131, pp. 2013-2015.
- Frankel, J.I.; Vick, B.; Ozisik, M.N.** (1985): Flux formulation of hyperbolic heat conduction, *Journal of Applied Physics*, Vol. 58, No. 9, pp. 3340-3345.
- Heidarinejad, G.; Shirmohammadi, R.; Maerefat, M.** (2008): Heat wave phenomena in solids subjected to time dependent surface heat flux, *Heat and Mass Transfer*, Vol. 44, No. 4, pp. 381-392.
- Hong, B.S.; Su, P.J.; Chou, C.Y.; Hung, C.I.** (2011): Realization of non-Fourier phenomena in heat transfer with 2D transfer function, *Applied Mathematical Modelling*, Vol. 35, pp. 4031-4043.
- Joseph, D.D.; Preziosi, L.** (1989): Heat waves, *Reviews of Modern Physics*, Vol.61,

No. 1, pp. 41-73.

**Kaminiski, W.** (1990): Hyperbolic heat conduction equation for materials with a nonhomogeneous inner structure, *ASME Journal of Heat Transfer*, Vol. 112, pp. 555-560.

**Lee, Z.Y.; Chen, C.K.; Hung, C.I.** (2002): Upper and lower bounds of the solution for an elliptic plate problem using a genetic algorithm, *Acta Mechanica*, Vol. 157, pp.201-212.

**Liu, K.C.; Chen H.T.** (2004): Numerical analysis for the hyperbolic heat conduction problem under a pulsed surface disturbances, *Applied Mathematics and Computation*, Vol. 159, No. 3, pp. 887-901.

**Maxwell, J.C.** (1867): On the dynamic theory of gases, *Philosophical Transactions of the Royal Society of London*, Vol. 157, pp. 49-88.

**Mitra, K.; Kumar, S.; Vedavarz, A.; Moallemi, M.K.** (1995): Experimental evidence of hyperbolic heat conduction in processed meat, *ASME Journal of heat transfer*, Vol. 117, No. 3, pp. 568-573.

**Nernst, W.** (1918): *Die Theoretischen und Experimentellen Grundlagen des Neuen Warmesatzes*, Knapp, Halle.

**Ni, J.H.; Chang, C.C.; Yang, Y.T.; Chen, C.K.** (2011): Surface heating problems of thermal propagation in living tissue solved by differential transformation method, *CMES: Computer Modeling in Engineering & Science*, Vol. 72, No. 1, pp. 37-51.

**Peng, H.S.; Chen, C.L.; Li, G..S.** (2012): Application of residual correction method to laser heating process, *International Journal of Heat and Mass Transfer*, Vol. 55, pp. 316-324.

**Peshkov, V.** (1914): Second sound in helium II, *Journal of Physics*, Vol. 8, pp. 381.

**Proter, M. H.; Weinberger, H. F.** (1967): *Maximum Principles in Differential Equations*, Prentice-Hall.

**Pourmohamadian, H.; Tabrizi, H.B.** (2007): Transient heat conduction for micro sphere, *4th WSEAS International Conference on Heat Mass Transfer*, Gold Coast, Queensland, Australia, January 17-19.

**Saedodin, S.; Torabi, M.** (2010): Electrical Discharge Machining (EDM) by using non-Fourier heat conduction model, *Contemporary Engineering Sciences*, Vol. 3, No. 6, pp. 269-283.

**Taitel, Y.** (1972): On the parabolic, hyperbolic and discrete formulation of the heat conduction equation, *International Journal of Heat and Mass Transfer*, Vol. 15, pp. 369-371.

**Tang, D.W.; Araki, N.** (1996): Non-Fourier heat conduction in a finite medium under periodic surface thermal disturbance, *International Journal of Heat and Mass Transfer*, Vol. 39, No. 8, pp. 1585-1590.

**Tang, H.W.; Chen, C.K. and Chiang, C.Y.** (2010): Application of residual correction method on error analysis of numerical solution on the non-Fourier fin problem, *CMES: Computer Modeling in Engineering & Science*, Vol. 65, No. 1, pp. 95-106.

**Tzou, D.Y.** (1997): *Macro- to Microscale Heat Transfer: The Lagging Behavior*, Taylor & Francis, Washington DC.

**Vermeersch, B.; Mey, G.D.** (2008): Non-fourier thermal conduction in nano-scaled electronic structures, *Analog Integrated Circuits and Signal Processing*, Vol. 55, No. 3, pp. 197-204.

**Vernotte, P.** (1961): Some possible complications in the phenomena of thermal conduction, *Compt. Rend. Acad. Sci.* 252, pp. 2190-2191.

**Wang, C.C.** (2006): Use residual correction method to calculate the upper and lower solutions of initial value problem, *Applied Mathematics and Computation*, Vol. 181, pp. 29-39.

**Wang, C.C.** (2007): Use of new residual correction method to calculate upper and lower solutions of natural convection, *Numerical Heat Transfer Part A*, Vol. 51, pp. 249-265.

**Wang, C.C.; Hu, H.P.** (2008): Study on monotonicity of boundary value problems of differential equations, *Applied Mathematics and Computation*, Vol. 202, pp. 383-394.

**Wang, C.C.** (2010): Applying the differential equation maximum principle with cubic spline method to determine the error bounds of forced convection problems, *International Communications in Heat and Mass Transfer*, Vol. 37, pp. 147-155.

**Xu, Y.S.; Guo, Z.Y.** (1995): Heat Wave Phenomena in IC Chips, *International Journal of Heat and Mass Transfer*, Vol. 38, No. 15, pp. 2919-2922.

